Multi-Functional Polymer Membranes Enable Integrated CO_2 Capture and Conversion in a Single, Continuous-Flow Membrane Reactor at Mild Conditions

Hui Xu,[1] Renxi Jin[2] and Casey P. O'Brien[2]*

[1]*Department of Chemistry and Biochemistry, University of Notre Dame, Notre Dame, IN, 46556, United Sates.*
[2]*Department of Chemical and Biomolecular Engineering, University of Notre Dame, Notre Dame, IN, 46556, United Sates.*

ABSTRACT: Herein, we present a membrane-based system designed to capture CO_2 from dilute mixtures and convert the captured CO_2 into value-added products in a single, integrated process operated continuously at mild conditions. Specifically, we demonstrate that quaternized poly(4-vinylpyridine) (P4VP) membranes are selective CO_2 separation membranes that are also catalytically active for cyclic carbonate synthesis from the cycloaddition of CO_2 to epichlorohydrin. We further demonstrate that quaternized P4VP membranes can integrate CO_2 capture, including from dilute mixtures down to 0.1 kPa CO_2, with CO_2 conversion to cyclic carbonates at 57 °C and atmospheric pressure. The catalytic membrane acts as both the CO_2 capture and conversion medium, providing an energy-efficient alternative to sorbent-based capture, compression, transport, and storage. The membrane is also potentially tunable for CO_2 conversion to a variety of products, including chemicals and fuels not limited to cyclic carbonates, which would be a transformative shift in carbon capture and utilization technology.

KEYWORDS: CO_2 capture, CO_2 conversion, integrated CO_2 capture and conversion, polymer membrane, catalytic membrane

INTRODUCTION

The Paris Agreement[1] set a goal to limit the global temperature increase to below 2 °C and preferably below 1.5 °C, relative to pre-industrial temperatures, to avoid catastrophic consequences of global warming. According to a recent Intergovernmental Panel on Climate Change (IPCC) special report,[2] limiting global warming to less than 2 °C will require widespread deployment of carbon capture technologies that capture CO_2 emissions from industrial processes (point source capture) or remove CO_2 directly from air (direct air capture), and either utilize it or store it permanently underground. However, current commercial carbon capture processes are sorbent-based technologies that are extremely inefficient and prohibitively expensive because they require energy-intensive regeneration stages to release CO_2 and regenerate the sorbent.[3, 4] Additionally, they produce CO_2 streams that must be compressed and transported to sites for utilization or storage, which reduces efficiency.

To reduce the energy intensity and costs associated with CO_2 capture, there is currently significant interest in the development of intensified processes that integrate CO_2 capture with CO_2 conversion to valuable products. For example, there are recent examples in the literature[5-16] of multifunctional catalytic materials with amine or alkali-metal hydroxide functional groups for capturing CO_2 from dilute streams such as flue gas or air, and catalytic sites (e.g., metals, halogens) for converting the captured CO_2 with H_2, steam, or epoxides to produce methane, formic acid, syngas (H_2 + CO), or cyclic carbonate products. While such multifunctional materials could improve the efficiency of CO_2 capture by eliminating the need to compress and transport high-pressure CO_2, these technologies require a two-step temperature-swing process to first capture CO_2 at low temperatures and then convert CO_2 at higher temperatures in a separate unit process (i.e., similar to sorbent-based carbon capture; see **Figure 1a**). A process that completely integrates the CO_2 capture and conversion processes in a single unit process could improve the energy efficiency of CO_2 capture even further.

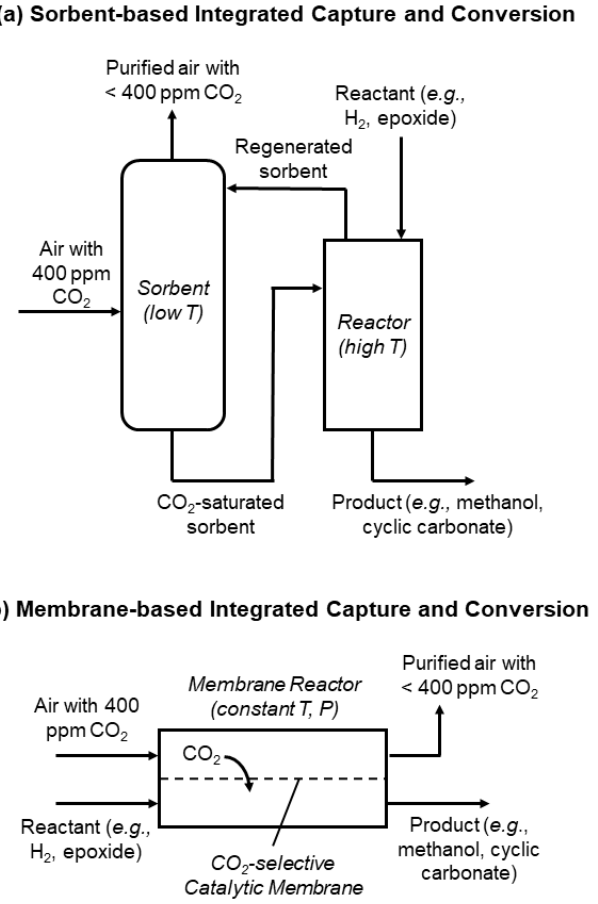

Figure 1. Schematic of (a) sorbent-based and (b) membrane-based integrated CO_2 capture and conversion.

Towards this end, this work introduces a multi-functional membrane concept that enables the integration of CO_2 capture from dilute sources with CO_2 conversion *in a single unit process operated continuously—not cyclical—at mild tem-*

peratures and pressures (see **Figure 1b**). The multi-functional membrane is polymeric with (a) amine groups attached to the polymer chain to selectively capture CO_2 from air or more concentrated point sources and facilitate CO_2 transport across the membrane via carbamate ($NCOO^-$) or bicarbonate (HCO_3^-) species;[17-24] and (b) catalytic groups (e.g., amines, halides, metals) to catalyze conversion of CO_2 on the permeate side of the membrane to value-added chemicals and/or fuels. The membrane ideally couples CO_2 transport across the membrane to CO_2 conversion on the permeate side through common molecular intermediates ($NCOO^-/HCO_3^-$) in both the transport and conversion processes.

In principle, the multi-functional membrane can couple CO_2 capture with any transformation that involves carbamate ($NCOO^-$) or bicarbonate (HCO_3^-) species including, but not limited to, cyclic carbonate synthesis from epoxides,[25-28] urea synthesis from NH_3,[29] methanol synthesis from H_2,[16, 30, 31] and formic acid from H_2O.[32] A key challenge is that the CO_2 capture and conversion processes occur in a single unit process and thus the operating conditions (e.g., temperature) for CO_2 capture and CO_2 conversion cannot be independently optimized but, rather, the operating conditions for both the CO_2 capture and conversion processes must be nearly identical. This is a significant challenge because CO_2 capture is typically carried out at low temperatures (<~70 °C) where CO_2 uptake is more favorable, but CO_2 conversion reactions are typically carried out at much higher temperatures.

Cyclic carbonate synthesis from the cycloaddition of CO_2 to epoxides is one particularly promising reaction for demonstrating the proof-of-principle and the potential of multi-functional polymer membranes for integrated CO_2 capture and conversion. Cyclic carbonate synthesis is: (*i*) thermodynamically favorable at mild temperatures and pressures; [33] (*ii*) known to be catalyzed by organic amines, including polymeric amines;[25-28, 34] (*iii*) believed to occur through carbamate and/or bicarbonate intermediates;[25-27, 34] and (*iv*) a 100% atom-economical "green" reaction that produces valuable cyclic carbonate products. Integrating CO_2 capture with more thermodynamically and kinetically challenging CO_2 conversion reactions, such as methanol synthesis, may require external stimulus (e.g., electricity, light) to enable operation at mild temperatures and pressures. Thus, cyclic carbonate synthesis is an ideal model reaction to demonstrate the proof-of-principle of multi-functional polymer membranes for integrating CO_2 capture and conversion because of its relative simplicity and thermodynamic and kinetic favorability of the reaction at mild temperatures.

To integrate CO_2 capture and conversion in a single unit process, a membrane is required that satisfies several criteria: (1) separates CO_2 from air or more concentrated point sources with high selectivity and permeability; (2) catalyzes CO_2 conversion on the permeate side of the membrane with high activity and selectivity at mild temperature and pressure; and (3) is stable for extended operation. In our previous work,[34] we demonstrated that poly(4-vinylpyridine) (P4VP), a polymer with pyridinic nitrogen groups attached to the polymer chain (see **Scheme 1**), is catalytically active for CO_2 cycloaddition to epoxides (epichlorohydrin) to give the corresponding cyclic carbonate product at mild temperature (57 °C) and atmospheric pressure (criterion 2). Further, P4VP membranes are permeable and selective to CO_2 separation from mixed gases (criterion 1).[35, 36] However, P4VP does not satisfy the third criterion (stability), and thus is not suitable for integrating CO_2 capture with CO_2 cycloaddition to epichlorohydrin, due to its high solubility in the epichlorohydrin reactant.

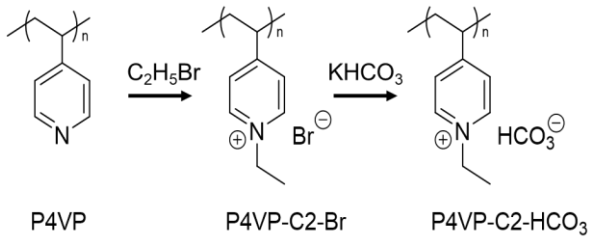

Scheme 1. Procedure for converting P4VP to bromoethane-quaternized P4VP (P4VP-C2-Br), and anion-exchange of P4VP-C2-Br with $KHCO_3$ to give P4VP-C2-HCO_3.

In this work, we demonstrate that synthetic quaternization of P4VP enhances the CO_2 separation performance, the catalytic activity, and the stability of the polymer in epichlorohydrin. We further demonstrate that P4VP-C2-HCO_3 membranes (see **Scheme 1**), synthesized by quaternization of P4VP with bromoethane (P4VP-C2-Br) followed by anion exchange of bromine with bicarbonate, can integrate CO_2 capture, including from extremely dilute CO_2/N_2 feed gas mixtures (0.1 kPa CO_2) similar to the concentration of CO_2 in air, with cyclic carbonate synthesis in a single membrane reactor unit operated continuously at mild temperature (57 °C) and atmospheric pressure. The P4VP-C2-HCO_3 material has not been reported in the literature to our knowledge. Other work has also shown that metal electrocatalytic functionality can be incorporated into P4VP-based materials for electrochemical CO_2 reduction, and polymer encapsulation of the metal catalyst can even enhance the activity, selectivity, and stability of the catalyst.[37-40] Thus, P4VP-based membranes are not only useful for demonstrating the proof-of-principle of the multi-functional polymer membrane concept for integrated CO_2 capture and conversion in a single unit process; they are also a highly tunable platform for integrating CO_2 capture with CO_2 conversion potentially to a variety of chemicals and fuels by incorporating metal electrocatalytic functionality into the membrane.

EXPERIMENTAL SECTION

Reagents. All chemicals were used as received without further purification: poly(4-vinylpyridine) (~160,000 MW, Sigma-Aldrich), bromoethane (VWR, ≥99.0%), dimethyl sulfoxide (TCI Chemicals, >99%), epichlorohydrin (VWR), 1,3,5-trimethoxybenzene (VWR, ≥99%), chloroform-d (VWR, ≥99.8%), potassium bicarbonate (Sigma-Aldrich, 99.7%), acetone (VWR, >99.5%), methanol (VWR, >99.8%). Polyvinylidene fluoride (PVDF) ultrafiltration substrates with a molecular weight cut off 100kDa were kindly donated by Philips' lab at the University of Notre Dame.

Synthesis of P4VP-C2-Br and P4VP-C2-HCO_3. Bromoethane-quaternized P4VP (P4VP-C2-Br; see **Scheme 1**) was

synthesized by first dissolving 1 g of P4VP in 12 mL of dimethyl sulfoxide at room temperature. Then 23.9 mmol of bromoethane was added into the mixture and the reaction was conducted at 50 °C for 2 days. After the reaction, the polymer was purified by precipitating in acetone. The final quaternized P4VP was dried in a vacuum oven for 2 days at room temperature. The degree of quaternization was ~100%, which was confirmed by ^{1}H NMR spectroscopy (**Figure S1**).

Synthesis of P4VP-C2-HCO_3 was carried out by anion-exchange of P4VP-C2-Br with $KHCO_3$. 0.4 g of P4VP-C2-Br was dissolved into methanol to prepare a 20 wt% solution. Then 4.6 mmol of $KHCO_3$ was added into the P4VP-C2-Br solution, and the mixture was stirred at room temperature for 48 h. After the reaction, the solution was filtered with a Nylon filter (size 0.45 μm) to remove the side product KBr. The structure of P4VP-C2-HCO_3 was confirmed using Attenuated Total Reflection Infrared (ATR-IR) spectroscopy. The ATR-FTIR measurements were performed using a Bruker Tensor 27 FTIR spectrometer, with a spectral resolution of 4 cm^{-1} and 64 scans-per-spectrum. The ATR-IR spectrum of P4VP-C2-HCO_3 (**Figure S2**) displayed bands associated with bicarbonate at 1673 cm^{-1}, 1399 cm^{-1}, 1278 cm^{-1}, and 1005 cm^{-1}, which were not present in the spectrum of P4VP-C2-Br. The band at 1673 cm^{-1} is close to the asymmetric stretch of C-O (~1650 cm^{-1}) in species HCO_3^- reported in the literature,[41] while the band at 1399 cm^{-1} is close to the symmetric stretch of C-O in bicarbonate (~1365 cm^{-1}).[41-43] Additionally, the band at 1278 cm^{-1} is close to the bending mode of C-OH in bicarbonate (~1300 cm^{-1}).[41, 43] The band at 1005 cm^{-1} is same as the asymmetric stretch of -C-OH in bicarbonate.[41, 43] The higher values of the asymmetric and symmetric stretch of-C-O, and the bending mode of C-OH in our study may be attributed to the presence of the pyridine ion, a conjugate cation whose π system may interact with the bicarbonate anion. Overall, these spectral assignments confirm the successful synthesis of P4VP-C2-HCO_3.

Preparation of P4VP, P4VP-C2-Br, and P4VP-C2-HCO_3 membranes. All the membranes utilized in this study were prepared by knife casting on PVDF substrates. Specifically, a 20 wt% methanol solution of P4VP-C2-HCO_3 was employed and directly cast onto a PVDF substrate with a certain wet thickness to fabricate the P4VP-C2-HCO_3 membranes. All membrane thickness values mentioned in this work are wet thicknesses. For the fabrication of P4VP-C2-Br membrane, a 20 wt% aqueous solution of P4VP-C2-Br was used, while a 20 wt% ethanol solution of P4VP was employed for the preparation of the P4VP membranes. Following the casting process, all membranes were left to dry overnight for subsequent analysis.

CO_2/N_2 separation performance measurements. All gas separation performance measurements were conducted with a gas permeation apparatus shown in **Figure S3**. The membranes were cut to 19 mm in OD and installed into the permeation cell. Aluminum gaskets were used on both sides of the membrane for sealing. The effective membrane surface area was determined to be ~1.77 cm^2. CO_2/N_2 gas mixtures with varying x% CO_2 and (100-x)% N_2 at a flow rate of 53 mL/min were used as the feed gas for permeation measurements. Ar with a flow rate of 10 mL/min was used as the sweep gas. The two streams were saturated with water vapor at 57 °C, and the feed and sweep were both at atmospheric pressure. The outlet gas compositions of the sweep side were analyzed by an online gas chromatograph (Agilent 7890) equipped with a Carboxen® 1010 PLOT capillary column and a TCD detector. CO_2 permeance and CO_2/N_2 selectivity were calculated from GC analysis of the permeate.

CO_2 cycloaddition reactivity measurements. The reactivity of P4VP, P4VP-C2-Br, and P4VP-C2-HCO_3 for CO_2 cycloaddition to epichlorohydrin was investigated using the batch reactor setup described in our previous study.[34] In this experimental configuration, a 25 mL Schlenk tube equipped with a gas bag was employed as the reactor. To commence the experimental procedure, 0.95 mmol of catalyst was introduced into the batch reactor, which was subsequently followed by the addition of a 5 mL solution of epichlorohydrin containing 0.1 g of 1,3,5-trimethoxybenzene, which was incorporated as the inner standard. After undergoing three cycles of CO_2 purging, a 1 L of pure CO_2 bag was connected to the reactor. The reaction was conducted at 57 °C under atmospheric pressure of CO_2 for 24 hours. Subsequently, the resulting solution was analyzed with ^{1}H NMR spectroscopy (Bruker AVANCE III HD 400 Nanobay spectrometer). Chloroform-d was used as the solvent for the ^{1}H NMR analysis.

Integrated CO_2 capture and conversion measurements. The apparatus used for integrated CO_2 capture and conversion measurements was the same as that used for gas separation performance measurements, except instead of using an Ar sweep, the epichlorohydrin reactant was cycled through the permeate side of the membrane (see **Figure 2**). In all the integrated CO_2 capture and conversion measurements, 5 mL of epichlorohydrin with 0.1 g of 1,3,5-trimethoxybenzene as the internal standard was used and cycled through the permeate side of the membrane with a VICI M6 pump. The epichlorohydrin was circulated through the reactor with a flux of 1000 μL/min. Same as the gas separation measurements, a water vapor-saturated gas mixture with x% CO_2 and (100- x)% N_2 with a total flow rate of 53 mL/min was used as the feed gas. After reacting at 57 °C for 24 h, the reaction solution was analyzed by ^{1}H-NMR spectroscopy using chloroform-d as the solvent.

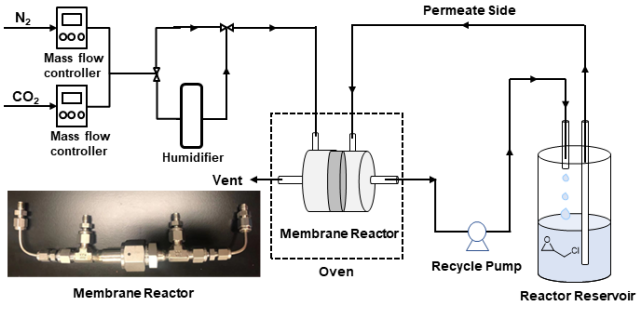

Figure 2. Schematic of the membrane reactor apparatus used for integrated CO_2 capture and conversion measurements.

RESULTS AND DISCUSSION

CO_2/N_2 separation performance of P4VP, P4VP-C2-Br and P4VP-C2-HCO_3. The CO_2 permeance and CO_2/N_2 selectivity of P4VP, P4VP-C2-Br and P4VP-C2-HCO_3 membranes with wet thicknesses of 0.356 mm were measured at 57°C and atmospheric pressure using a permeation apparatus depicted in **Figure S3**. The feed gas employed for the experiments consisted of 15% CO_2 and 85% N_2 (dry basis), which was saturated with water vapor by passing through a water bubbler. The sweep gas was pure Ar, which was also saturated with water vapor using a bubbler. To ensure reliable and accurate measurements, three membrane samples were evaluated for each material. The CO_2 permeance and CO_2/N_2 selectivity of the P4VP, P4VP-C2-Br and P4VP-C2-HCO_3 membranes are summarized in **Figure 3**.

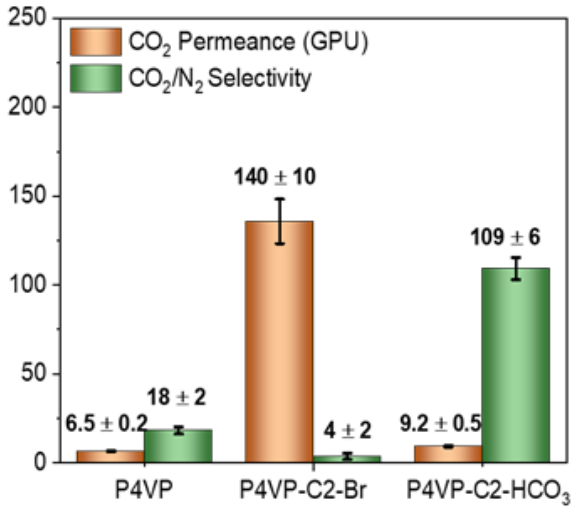

Figure 3. Comparison of the CO_2 permeance (orange) and CO_2/N_2 selectivity (green) of P4VP, P4VP-C2-Br, and P4VP-C2-HCO_3 membranes (Conditions: feed side: humidified 15% CO_2 and 85% N_2 (dry basis) with a total flow rate of 53 mL/min, 1 atm; sweep side: humidified Ar with a flow rate of 10 mL/min, 1 atm; 57 °C). Each data point represents the average of three membranes.

The CO_2 permeance of P4VP was 6.5 ± 0.2 GPU, with a CO_2/N_2 selectivity of 18 ± 2. The CO_2 permeance of P4VP-C2-Br (140 ± 10 GPU) was significantly higher, but the CO_2/N_2 selectivity of P4VP-C2-Br (4 ± 2) was significantly lower, than that of P4VP. To understand the underlying cause of the reduced CO_2/N_2 selectivity exhibited by P4VP-C2-Br membranes at 57 °C, gas separation measurements were conducted at room temperature. The results (**Figure S4a**) show that the CO_2/N_2 selectivity reached 57 ± 8. However, upon increasing the temperature to 57 °C (**Figure S4b**), the CO_2/N_2 selectivity decreased to 5.6 ± 0.2. The reason for the decrease in the CO_2/N_2 selectivity of P4VP-C2-Br membranes at 57°C is not clear, but it could be due to the dissolution of P4VP-C2-Br in water vapor at this elevated temperature.

To improve the thermal stability of the P4VP-C2-Br membrane, an ion exchange process was employed to substitute the bromide counter ion with bicarbonate ions (see **Scheme 1**). This strategy was based on the hypothesis that bicarbonate ions could engage in hydrogen bonding interactions, thereby improving the overall stability of the membrane. Additionally, the use of bicarbonate ions offers environmental advantages over bromide ions, bicarbonate ions are reactive towards epoxides,[44] and bicarbonate ions were reported as key intermediates in coupled CO_2 capture and conversion.[45-47] The ion exchange process was carried out using $KHCO_3$ as the exchange agent (see **Experimental Section**).

The replacement of bromide with bicarbonate as the counter ion yielded noteworthy improvements in the CO_2/N_2 selectivity of the membrane (see **Figure 3**). Specifically, at 57 °C, the CO_2/N_2 selectivity increased significantly from 4 ± 2 for P4VP-C2-Br to 109 ± 6 for P4VP-C2-HCO_3. This substantial enhancement in the CO_2/N_2 selectivity clearly indicates the superior performance of the P4VP-C2-HCO_3 membrane compared to both P4VP-C2-Br and P4VP in terms of selective separation of CO_2 and N_2. The enhanced CO_2/N_2 selectivity of P4VP-C2-HCO_3 at 57 °C compared to P4VP-C2-Br may be related to the ability of bicarbonate ions to engage in hydrogen bonding interactions that may enhance its thermal stability, as hypothesized above, or the lower water solubility of P4VP-C2-HCO_3. The lower CO_2 permeance, but higher CO_2/N_2 selectivity, of P4VP-C2-HCO_3 compared to P4VP-C2-Br is most likely related to the well-known "permeability-selectivity tradeoff" inherent to polymer membrane separations[48-50]: membranes that are more permeable are generally less selective, and vice-versa.

In order to comprehensively evaluate the gas separation performance of P4VP-C2-HCO_3, the CO_2 permeance and CO_2/N_2 selectivity of P4VP-C2-HCO_3 was measured as a function of CO_2 partial pressure from 0.1 kPa (i.e., similar to the CO_2 concentration in air) up to 86 kPa. As shown in **Figure 4**, the CO_2 permeance and CO_2/N_2 selectivity increase with decreasing CO_2 partial pressure, which suggests that the P4VP-C2-HCO_3 membrane behaves like a facilitated transport membrane.[51-53] Notably, at a low CO_2 partial pressure of approximately 0.1 kPa, the P4VP-C2-HCO_3 membrane exhibited a high CO_2 permeance of 1300 ± 100 GPU and a high CO_2/N_2 selectivity of 3000 ± 1000. The high uncertainty in the CO_2/N_2 selectivity measurement at 0.1 kPa is likely due to the small amount of CO_2 in the permeate stream at this pressure, and hence the relatively low signal-to-noise ratio of the CO_2 peak in gas chromatography. These results indicate that the P4VP-C2-HCO_3 membrane is effective at separating CO_2 from gas mixtures under conditions that closely resemble atmospheric compositions.

P4VP membranes exhibited a similar trend of increasing CO_2 permeance and CO_2/N_2 selectivity with decreasing CO_2 partial pressure (**Figure S5**), but with a lower CO_2 permeance and CO_2/N_2 selectivity compared to P4VP-C2-HCO_3. The CO_2 permeance and CO_2/N_2 selectivity of P4VP-C2-Br was not evaluated as a function of CO_2 partial pressure at 57 °C due to its poor thermal stability, as discussed above.

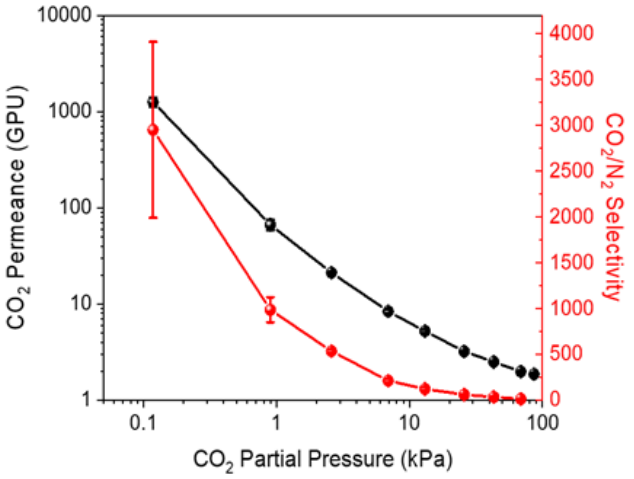

Figure 4. CO_2 permeance (black; left axis) and CO_2/N_2 selectivity (red; right axis) of P4VP-C2-HCO_3 versus feed CO_2 partial pressure (Conditions: feed side: humidified x % CO_2 and $(100 - x)$ % N_2 (dry basis) with a total flow rate of 53 mL/min, 1 atm; sweep side: humidified Ar with a flow rate of 10 mL/min, 1 atm; 57 °C). Each data point represents the average of three membranes.

CO_2 cycloaddition reactivity of P4VP, P4VP-C2-Br, and P4VP-C2-HCO_3. The catalytic performance of P4VP, P4VP-C2-Br, and P4VP-C2-HCO_3 for the CO_2 cycloaddition reaction was evaluated at 57 °C and 1 atm CO_2 for 24 h using a batch reactor setup described previously (see **Figure S6**).[34] By comparing the ^{1}H NMR spectra of the epichlorohydrin solution before and after the reaction involving P4VP, P4VP-C2-Br (**Figure S7**), and P4VP-C2-HCO_3 (**Figure S8**), distinct peaks emerged that were identified as cyclic carbonate, verified through comparison with the ^{1}H NMR spectrum of the cyclic carbonate (**Figure S9**). Thus, both P4VP-C2-Br and P4VP-C2-HCO_3 exhibit catalytic activity in the cycloaddition reaction between CO_2 and epichlorohydrin at mild temperatures and CO_2 pressures. Trace amounts of diols, with characteristic ^{1}H NMR peaks at 3.75-4 ppm, were also observed.

The production rate of cyclic carbonate was calculated for P4VP, P4VP-C2-Br, and P4VP-C2-HCO_3 for comparison. The production rate is reported in mmol of product per hour per reactive site, where we assume that there is one active site per pyridine unit in each polymeric material. **Figure 5** shows the cyclic carbonate production rate of P4VP, P4VP-C2-Br, and P4VP-C2-HCO_3. The results show that, while the cyclic carbonate production rate is similar for the three materials, P4VP-C2-HCO_3 exhibited a significantly higher cyclic carbonate production rate (10.3 ± 0.6 mmol/h/active site) compared to P4VP-C2-Br (6.9 ± 0.6 mmol/h/active site) and P4VP (8.0 ± 0.3 mmol/h/active site). The similarity in the catalytic activity of P4VP, P4VP-C2-Br, and P4VP-C2-HCO_3 may suggest that the active sites in these different materials is similar, and the activity of this site is sensitive to quaternization and anion-exchange, which may influence the reaction mechanism directly or indirectly (by influencing the electronic structure of the active site, for example). Nevertheless, these results show that catalytic activity of P4VP can be tuned and enhanced by synthetic quaternization.

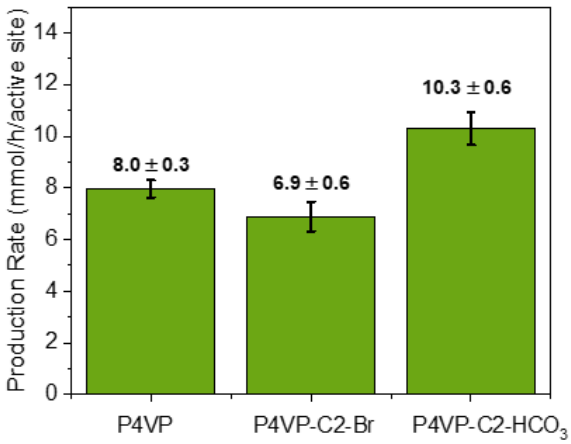

Figure 5. Comparison of the cyclic carbonate production rate of P4VP, P4VP-C2-Br, and P4VP-C2-HCO_3 in the batch reactor under 1 atm CO_2 at 57 °C after reaction for 24 h. Each data point represents the average and standard deviation of four batches.

Integrated CO_2 capture and conversion using P4VP-C2-HCO_3. Our CO_2/N_2 separation performance measurements and CO_2 cycloaddition activity measurements show that P4VP-C2-HCO_3 is selective for CO_2/N_2 separation at 57 °C; is active for the CO_2 cycloaddition reaction at 57 °C; and is insoluble in the epichlorohydrin reactant. P4VP and P4VP-C2-Br, on the other hand, do not satisfy these criteria for selecting a membrane for integrated CO_2 capture and conversion to cyclic carbonates because P4VP is solubilized by epichlorohydrin, and P4VP-C2-Br is not selective for CO_2/N_2 separation at 57 °C. Thus, P4VP-C2-HCO_3 is the most promising membrane in this study for integrating CO_2 capture and conversion to cyclic carbonates.

The integration of CO_2 capture with CO_2 conversion to cyclic carbonates was evaluated in the membrane reactor (**Figure 2**) using a P4VP-C2-HCO_3 membrane with a wet thickness of 0.356 mm. The procedure for testing the overall rate of integrated CO_2 capture and conversion using the P4VP-C2-HCO_3 membrane initially involved verifying its CO_2/N_2 selectivity through gas separation performance testing. The testing was performed using a feed gas consisting of 15% CO_2, 85% N_2 (dry basis) saturated with water vapor with a total dry gas (CO_2 and N_2) flow rate of 53 mL/min at atmospheric pressure. After verifying the CO_2/N_2 selectivity of the membrane, the integration of CO_2 capture and CO_2 conversion to cyclic carbonates was then investigated by changing the sweep from Ar to epichlorohydrin containing 1,3,5-trimethoxybenzene as an inner standard without changing the feed side setup. The composition of the reaction solution containing the epichlorohydrin reactant and the cyclic carbonate produced from the reaction was monitored with ^{1}H NMR in $CDCl_3$. ^{1}H NMR results (see **Figure S10**) indicate that a significant amount of cyclic carbonate was produced during integrated CO_2 capture and conversion using P4VP-C2-HCO_3. This confirms that P4VP-C2-HCO_3 can effectively capture CO_2 from mixed gas streams and convert the captured CO_2 to cyclic carbonate in a single, continuous unit

process at mild temperatures (57 °C) and atmospheric pressure.

To further investigate the role of the P4VP-C2-HCO_3 membrane in the CO_2 capture and conversion process, a control experiment was conducted using the batch reactor with the P4VP-C2-HCO_3 membrane as the catalyst. The reaction conditions and gas composition were kept the same as in the membrane reactor system used for integrated CO_2 capture and conversion to mimic the conditions in the membrane reactor. The membrane was suspended in the batch reactor at the gas-liquid interface, identical to its position in the membrane reactor (**Figure S11**). To simulate water vapor in the CO_2/N_2 feed, 113 μL of DI water (see Section S3 for calculation) was added to the liquid, and 1L of simulated flue gas (15% CO_2 and 85% N_2) was introduced into the reactor. The reaction was carried out at 57 °C and sampled at certain time intervals up to 48 hours. The time-resolved ^{1}H NMR spectra of the reaction solution with the membrane at the gas-liquid interface is shown in **Figure S12b**. The ^{1}H NMR results show that there was not a significant amount of cyclic carbonate produced during the 48-hour of reaction in the control experiment using a batch reactor with the P4VP-C2-HCO_3 membrane as the catalyst.

An additional control experiment was conducted in the batch reactor under the same conditions, with the exception that the membrane was immersed in the epichlorohydrin liquid (**Figure S13**). The resulting ^{1}H NMR spectra are presented in **Figure S14**, and similarly, only trace amounts of cyclic carbonate were detected. Therefore, we can conclude that the P4VP-C2-HCO_3 plays a crucial role in separating CO_2 from the CO_2/N_2 gas mixture and delivering concentrated CO_2 to the catalytically active sites of the membrane at the gas-solid-liquid interface for conversion with epichlorohydrin to cyclic carbonate. Additionally, the membrane acts as a barrier preventing evaporation of the volatile epichlorohydrin reactant.

The influence of membrane thickness and CO_2 partial pressure on the rate of integrated CO_2 capture and conversion using P4VP-C2-HCO_3. To investigate the influence of membrane thickness on the CO_2/N_2 separation performance and the integrated CO_2 capture and conversion process, P4VP-C2-HCO_3 membranes with varying wet thicknesses from 0.178 mm to 0.712 mm were prepared and evaluated in the membrane reactor apparatus. We are not necessarily limited to membranes in the wet thickness range of 0.178 to 0.712 mm, but membranes thinner than 0.178 mm wet thickness are difficult to prepare reproducibly.

As expected, the CO_2 flux (**Figure 6**, green bars, left axis) and the CO_2 permeance (**Figure S15**) decreased monotonically with increasing P4VP-C2-HCO_3 membrane thickness. The CO_2/N_2 selectivity of P4VP-C2-HCO_3 increased as the membrane wet thickness increased from 0.178 mm (65 ± 7) to 0.356 mm (150 ± 20), as expected, and then decreased to 109 ± 4 as the membrane wet thickness increased further to 0.712 mm (**Figure S15**). This non-monotonic trend in the CO_2/N_2 selectivity of P4VP-C2-HCO_3 is surprising as selectivity in facilitated transport membranes is expected to increase with increasing membrane thickness.[51] The origin of this unexpected trend is not clear, but the CO_2/N_2 selectivity of P4VP-C2-HCO_3 is still quite high in the 0.178 to 0.712 mm wet thickness range.

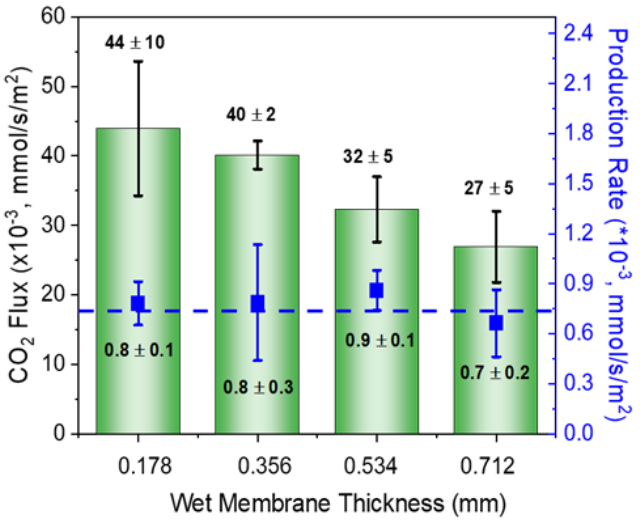

Figure 6. Comparison of the CO_2 flux (green bars; left axis) and cyclic carbonate production rate (blue data points; right axis) during integrated CO_2 capture and conversion with different membrane wet thicknesses. (Feed gas composition: 15% CO_2 and 85% N_2 (dry basis) with a total flow rate of 53 mL/min, water vapor saturated, 1 atm; sweep side: humidified Ar at a flow rate of 10 mL/min, 1 atm; 57 °C; reaction temperature: 57 °C; reaction time: 24 hours). Each data point represents the average and standard deviation of three different membranes.

The overall rate of integrated CO_2 capture and conversion to cyclic carbonates using P4VP-C2-HCO_3 membranes with different membrane thickness is shown in **Figure 6** (blue data points; right axis). The overall rate of cyclic carbonate production remains roughly constant at (7.7 ± 0.8) × 10^{-4} mmol/s/m^2 as the membrane wet thickness increases from 0.178 mm to 0.712 mm. If CO_2 transport across the membrane was the rate-limiting step in the overall CO_2 capture and conversion sequence, then one would expect the cyclic carbonate production rate to decrease with increasing membrane thickness, similar to the trend observed in the CO_2 flux (**Figure 6**, green bars, left axis). The observation that the cyclic carbonate production rate is independent of the membrane thickness suggests that the rate-limiting step in the combined CO_2 capture and conversion process is the conversion of CO_2 to cyclic carbonates. This conclusion is further supported by our observation that the CO_2 fluxes across the P4VP-C2-HCO_3 membranes are more than an order-of-magnitude larger than the rate of integrated CO_2 capture and conversion to cyclic carbonates.

The performance of P4VP-C2-HCO_3 for integrated CO_2 capture and conversion was further evaluated by examining its performance under varied CO_2 partial pressures, using P4VP-C2-HCO_3 membranes with a wet thickness of 0.356 mm. **Figure 7** shows that the CO_2 flux across the membrane increases as the feed CO_2 partial pressure increases from 0.1 kPa to 86 kPa, as expected. Additionally, while there is a relatively large uncertainty in the cyclic carbonate production

rate measured at 15 kPa CO_2, there is a general trend of increasing rate of cyclic carbonate production with increasing CO_2 partial pressure. As our membrane thickness-dependent measurements (**Figure 6**) suggest that conversion of CO_2 to cyclic carbonates is the rate-limiting step in the combined CO_2 capture and conversion process, the increase in the cyclic carbonate production rate with increasing CO_2 partial pressure is most likely due to an increase in the concentration of dissolved CO_2 in the membrane, and not necessarily due to an increase in the CO_2 flux across the membrane. It is also noteworthy that P4VP-C2-HCO_3 exhibited the ability to capture and convert CO_2 into cyclic carbonate even at extremely low CO_2 partial pressures of 0.1 kPa (0.1%), which is close to the CO_2 partial pressure in air (0.04 kPa). Thus, the catalytic membrane is promising for direct air capture and conversion of CO_2.

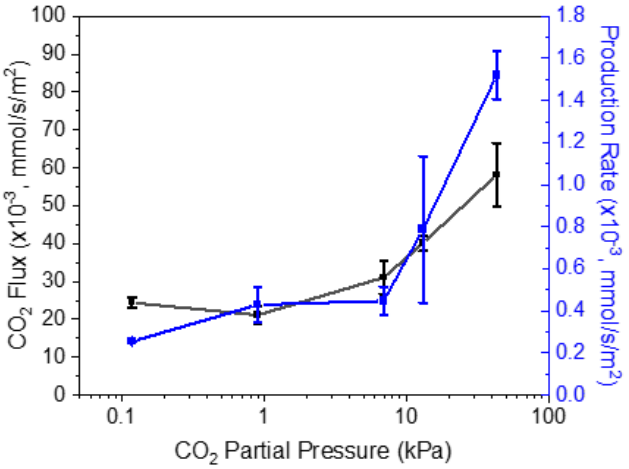

Figure 7. CO_2 flux (black; left axis) and cyclic carbonate production rate (blue; right axis) of P4VP-C2-HCO_3 versus feed CO_2 partial pressure in the integrated CO_2 capture and conversion system. (Membrane wet thickness: 0.356 mm; feed gas composition: x% CO_2 and $(100-x)$% N_2 (dry basis) with a total flow rate of 53 mL/min, water vapor-saturated, 1 atm; sweep side: humidified Ar at a flow rate of 10 mL/min, 1 atm; 57 °C; reaction temperature: 57 °C; reaction time: 24 h). Each data point represents the average and standard deviation of three different membranes.

Stability of P4VP-C2-HCO_3 during integrated CO_2 capture and conversion. The stability of the P4VP-C2-HCO_3 membrane during integrated CO_2 capture and conversion to cyclic carbonates was evaluated by measuring the cyclic carbonate production rate as a function of time from 0 to 48 h of reaction. The results, presented in **Figure S16a**, show that the cyclic carbonate production rate decreased from an initial value of ~2.8 × 10^{-3} mmol/s/m^2 to a nearly constant value of ~1 × 10^{-3} mmol/s/m^2 at reaction times greater than ~30 h.

To investigate the underlying reason for the decrease in the cyclic carbonate production rate over time, the P4VP-C2-HCO_3 membrane was analyzed by ATR-FTIR spectroscopy before and after the reaction. The ATR-FTIR results, presented in **Figure S17**, revealed small but significant changes in several FTIR bands over the course of the reaction. We postulate that the decrease in membrane reactivity may be attributed to the formation of byproducts, such as glycidol or 3-chloro-1,2-propanediol, that may adsorb strongly on the membrane surface. The strong OH stretch[54-56] band observed at approximately 3301 cm^{-1} and the shift in the asymmetric stretch of C-OH in bicarbonate from 1005 cm^{-1} to 1043 cm^{-1} could be evidence of this deactivation. Additionally, the band observed at 1043 cm^{-1} may also contribute to the shift of C-O groups in 3-chloro-1,2-propanediol (which is normally observed at ~1031 cm^{-1}).[54] These observations may suggest that byproducts such as 3-chloro-1,2-propanediol are bound to the membrane surface rather than in solution. These byproducts may block active sites on the P4VP-C2-HCO_3 membrane surface, thereby decreasing the rate of conversion of CO_2 to cyclic carbonate, which was determined to be the rate-limiting step in the combined CO_2 capture and conversion process. The presence of these potential byproducts may be difficult to distinguish via ^{1}H NMR because of their low concentrations and adsorption on the membrane, although peaks were detected at 3.75-4 ppm.

In addition to a decrease of the production rate of cyclic carbonate over reaction time, the CO_2/N_2 selectivity of P4VP-C2-HCO_3 was also compromised by exposure to the epichlorohydrin reaction mixture, as depicted in **Figure S16b**. Prior to exposure to epichlorohydrin, the CO_2/N_2 selectivity of P4VP-C2-HCO_3 was 109 ± 6, which decreased to 5 ± 5 after epichlorohydrin exposure. The CO_2 flux across P4VP-C2-HCO_3 is quite stable prior to exposure to the epichlorohydrin reactant, during exposure to humidified 15% CO_2 / 85% N_2 (dry basis) with a humidified Ar sweep (**Figure S18**). This suggests that the integrity of the membrane might have been compromised during the reaction from exposure to epichlorohydrin and potentially stemming from the formation of byproducts such as glycidol or 3-chloro-1,2-propanediol. Another plausible cause for the compromised membrane integrity is the dissolution of the membrane in the epichlorohydrin reaction solution, which has the potential to induce structural damage to the membrane.

Based on our results and a mechanism reported in the literature for bicarbonate-catalyzed cyclic carbonate synthesis,[57] the proposed reaction mechanism of P4VP-C2-HCO_3, including formation of byproducts, is illustrated in **Figure 8**. The bicarbonate counter ion in the membrane opens the epoxide ring of epichlorohydrin to form intermediate **I**. Then, the intermediate **I** can attack CO_2 to form intermediate **II**, and further release the desired product (cyclic carbonate) and reform bicarbonate ion, which can further react with epoxide and CO_2 to form the desired product. Besides the desired reaction process, the intermediate **I** may also form the intermediate **III** and intermediate **IV**, which can be further converted to side products glycidol and 3-chloro-1,2-propanediol. As mentioned previously, although the P4VP-C2-HCO_3 membrane is more selective for CO_2/N_2 separation than P4VP-C2-Br at 57 °C, the stability towards the epichlorohydrin reactant still needs to be improved by further materials research and development.

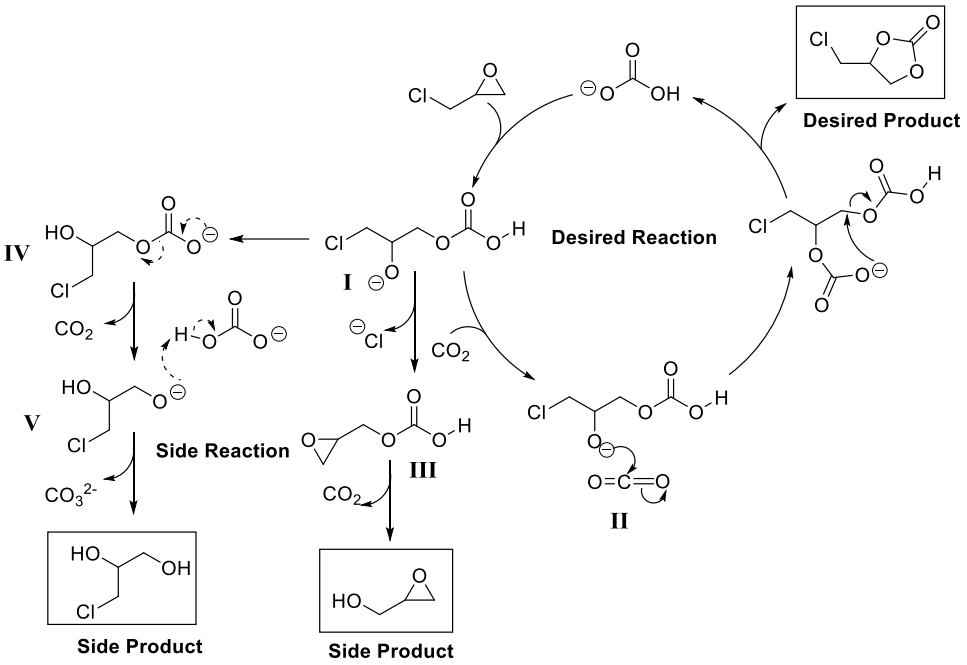

Figure 8. Proposed mechanism of the CO_2 capture and conversion process, including the formation of byproducts.

CONCLUSIONS

This work demonstrates that synthetically-quaternized P4VP membranes are a promising and tunable platform for integrating CO_2 capture and conversion in a single, continuous process at mild conditions. Remarkably, the P4VP-C2-HCO_3 membrane system can capture and convert CO_2 even from streams with low CO_2 concentration (such as 0.1 kPa), which is approximately the CO_2 concentration to air. Thus, this work provides a promising approach for direct CO_2 capture and conversion, opening new opportunities in this field. While this work focuses on CO_2 conversion to cyclic carbonates as a model system, due to its relative simplicity and the thermodynamic and kinetic favorability of this reaction at mild temperatures, the catalytic membrane is potentially tunable for CO_2 conversion to a variety of chemicals and/or fuels by incorporating metal electrocatalytic functionality into the membrane, for example. If the technology is capable of being sufficiently scaled up, this would be a transformative shift in carbon capture and utilization technology that could have a large impact on chemical engineering in the future.

ASSOCIATED CONTENT

Supporting Information

The supporting Information is available free of charge on the ACS Publications website.

^{1}H NMR spectra, ATR-IR spectra, membrane reactor and batch reactor apparatus schematics, P4VP-C2-Br membrane performance at room temperature and 57 °C, P4VP membrane performance versus CO_2 partial pressure, water calculation, P4VP-C2-HCO_3 membrane performance versus membrane thickness, P4VP-C2-HCO_3 membrane stability.

AUTHOR INFORMATION

Corresponding Author

* Casey P. O'Brien: Department of Chemical and Biomolecular Engineering, University of Notre Dame, Notre Dame, Indiana 46556, United States. Email: cobrie23@nd.edu

Author Contributions

All authors have given approval to the final version of the manuscript.

ACKNOWLEDGMENT

This work was funded through U.S. national Science Foundation CAREER award [CBET-2144362]. We thank the Center for Environmental Science and Technology (CEST) for the use of ATR-FTIR. We thank Professor William Phillip's group for providing the PVDF support membranes.

REFERENCES

(1) Horowitz, C. A. Paris Agreement. *International Legal Materials* **2017**, *55* (4), 740-755.
(2) IPCC. *Global Warming of 1.5 ºC*. 2018. https://www.ipcc.ch/sr15/
(3) National Academies of Sciences, E., Medicine. *Negative Emissions Technologies and Reliable Sequestration: A Research Agenda*; The National Academies Press, 2019.
(4) Ozkan, M. Direct Air Capture of CO_2: A Response to Meet the Global Climate Targets. *MRS Energy & Sustainability* **2021**, *8* (2), 51-56.
(5) Maina, J. W.; Pringle, J. M.; Razal, J. M.; Nunes, S.; Vega, L.; Gallucci, F.; Dumée, L. F. Strategies for Integrated Capture and Conversion of CO_2 from Dilute Flue Gases and the Atmosphere. *ChemSusChem* **2021**, *14* (8), 1805-1820.
(6) Chen, J.; Xu, Y.; Liao, P.; Wang, H.; Zhou, H. Recent Progress in Integrated CO_2 Capture and Conversion Process Using Dual

Function Materials: A State-of-the-Art Review. *Carbon Capture Science & Technology* **2022**, *4*, 100052.
(7) Sun, S.; Sun, H.; Williams, P. T.; Wu, C. Recent Advances in Integrated CO_2 Capture and Utilization: A Review. *Sustainable Energy & Fuels* **2021**, *5* (18), 4546-4559, 10.1039/D1SE00797A.
(8) Pazdera, J.; Berger, E.; Lercher, J. A.; Jentys, A. Conversion of CO_2 to Methanol over Bifunctional Basic-Metallic Catalysts. *Catalysis Communications* **2021**, *159*, 106347.
(9) Jakobsen, J. B.; Rønne, M. H.; Daasbjerg, K.; Skrydstrup, T. Are Amines the Holy Grail for Facilitating CO_2 Reduction? *Angew. Chem. Int. Ed.* **2021**, *60* (17), 9174-9179.
(10) Zanatta, M.; García-Verdugo, E.; Sans, V. Direct Air Capture and Integrated Conversion of Carbon Dioxide into Cyclic Carbonates with Basic Organic Salts. *ACS Sustain. Chem. Eng.* **2023**, *11* (26), 9613-9619.
(11) Kim, S. M.; Abdala, P. M.; Broda, M.; Hosseini, D.; Copéret, C.; Müller, C. Integrated CO_2 Capture and Conversion as an Efficient Process for Fuels from Greenhouse Gases. *ACS Catal.* **2018**, *8* (4), 2815-2823.
(12) Sasayama, T.; Kosaka, F.; Liu, Y.; Yamaguchi, T.; Chen, S.-Y.; Mochizuki, T.; Urakawa, A.; Kuramoto, K. Integrated CO_2 Capture and Selective Conversion to Syngas Using Transition-Metal-Free Na/Al_2O_3 Dual-Function Material. *J. CO2 Util.* **2022**, *60*, 102049.
(13) Barthel, A.; Saih, Y.; Gimenez, M.; Pelletier, J. D. A.; Kühn, F. E.; D'Elia, V.; Basset, J.-M. Highly Integrated CO_2 Capture and Conversion: Direct Synthesis of Cyclic Carbonates from Industrial Flue Gas. *Green Chemistry* **2016**, *18* (10), 3116-3123, 10.1039/C5GC03007B.
(14) Yi, Q.; Liu, T.; Wang, X.; Shan, Y.; Li, X.; Ding, M.; Shi, L.; Zeng, H.; Wu, Y. One-Step Multiple-Site Integration Strategy for CO_2 Capture and Conversion into Cyclic Carbonates under Atmospheric and Cocatalyst/Metal/Solvent-Free Conditions. *Applied Catalysis B: Environmental* **2021**, *283*, 119620.
(15) Ma, H.; Liu, S.; Wang, H.; Li, G.; Zhao, K.; Cui, X.; Shi, F. In Situ CO_2 Capture and Transformation into Cyclic Carbonates using Flue Gas. *Green Chemistry* **2023**, *25* (6), 2293-2298, 10.1039/D2GC04757H.
(16) Kar, S.; Goeppert, A.; Prakash, G. K. S. Integrated CO_2 Capture and Conversion to Formate and Methanol: Connecting Two Threads. *Accounts of chemical research* **2019**, *52* (10), 2892-2903.
(17) Xu, H.; Pate, S. G.; O'Brien, C. P. The Influence of Amine Structure on the Mechanism of CO_2 Facilitated Transport across Amine-Functionalized Polymer Membranes: An *Operando* Spectroscopy Study. *J. Membr. Sci.* **2024**, *689*, 122163.
(18) Xu, H.; Pate, S. G.; O'Brien, C. P. Mathematical Modeling of CO_2 Facilitated Transport across Polyvinylamine Membranes with Direct Operando Observation of Amine Carrier Saturation. *Chem. Eng. J.* **2023**, *460*, 141728.
(19) Tong, Z.; Ho, W. S. W. Facilitated Transport Membranes for CO_2 Separation and Capture. *Sep. Sci. Technol.* **2017**, *52* (2), 156-167.
(20) Deng, L.; Kim, T.-J.; Hägg, M.-B. Facilitated Transport of CO_2 in Novel PVAm/PVA Blend Membrane. *J. Membr. Sci.* **2009**, *340* (1), 154-163.
(21) Rafiq, S.; Deng, L.; Hägg, M.-B. Role of Facilitated Transport Membranes and Composite Membranes for Efficient CO_2 Capture – A Review. *ChemBioEng Rev.* **2016**, *3* (2), 68-85.
(22) Huang, J.; Zou, J.; Ho, W. S. W. Carbon Dioxide Capture Using a CO_2-Selective Facilitated Transport Membrane. *Ind. Eng. Chem. Res.* **2008**, *47*, 1261-1267.
(23) Xu, H.; Easa, J.; Pate, S. G.; Jin, R.; O'Brien, C. P. Operando Surface-Enhanced Raman-Scattering (SERS) for Probing CO_2 Facilitated Transport Mechanisms of Amine-Functionalized Polymeric Membranes. *ACS Appl. Mater. Interfaces* **2022**, *14* (13), 15697-15705.
(24) Pate, S. G.; Xu, H.; O'Brien, C. P. Operando Observation of CO_2 Transport Intermediates in Polyvinylamine Facilitated Transport Membranes, and the Role of Water in the Formation of Intermediates, Using Transmission FTIR Spectroscopy. *J. Mater. Chem. A* **2022**, *10* (8), 4418-4427, 10.1039/D1TA10015G.
(25) Srivastava, R.; Srinivas, D.; Ratnasamy, P. Sites for CO_2 Activation over Amine-Functionalized Mesoporous Ti(Al)-SBA-15 Catalysts. *Microporous and Mesoporous Materials* **2006**, *90* (1), 314-326.
(26) Wei-Li, D.; Bi, J.; Sheng-Lian, L.; Xu-Biao, L.; Xin-Man, T.; Chak-Tong, A. Novel Functionalized Guanidinium Ionic Liquids: Efficient Acid–Base Bifunctional Catalysts for CO_2 Fixation with Epoxides. *Journal of Molecular Catalysis A: Chemical* **2013**, *378*, 326-332.
(27) Zhang, X.; Zhao, N.; Wei, W.; Sun, Y. Chemical Fixation of Carbon Dioxide to Propylene Carbonate over Amine-Functionalized Silica Catalysts. *Catal. Today* **2006**, *115* (1), 102-106.
(28) Yu, K. M. K.; Curcic, I.; Gabriel, J.; Morganstewart, H.; Tsang, S. C. Catalytic Coupling of CO_2 with Epoxide Over Supported and Unsupported Amines. *The Journal of Physical Chemistry A* **2010**, *114* (11), 3863-3872.
(29) Manaka, Y.; Nagatsuka, Y.; Motokura, K. Organic Bases Catalyze the Synthesis of Urea from Ammonium Salts Derived from Recovered Environmental Ammonia. *Sci. Rep.* **2020**, *10* (1), 2834.
(30) Kothandaraman, J.; Goeppert, A.; Czaun, M.; Olah, G. A.; Prakash, G. K. S. Conversion of CO_2 from Air into Methanol Using a Polyamine and a Homogeneous Ruthenium Catalyst. *J. Am. Chem. Soc.* **2016**, *138* (3), 778-781.
(31) Kar, S.; Sen, R.; Goeppert, A.; Prakash, G. K. S. Integrative CO_2 Capture and Hydrogenation to Methanol with Reusable Catalyst and Amine: Toward a Carbon Neutral Methanol Economy. *J. Am. Chem. Soc.* **2018**, *140* (5), 1580-1583.
(32) Pérez-Gallent, E.; Vankani, C.; Sánchez-Martínez, C.; Anastasopol, A.; Goetheer, E. Integrating CO_2 Capture with Electrochemical Conversion Using Amine-Based Capture Solvents as Electrolytes. *Ind. Eng. Chem. Res.* **2021**, *60* (11), 4269-4278.
(33) Guo, L.; Lamb, K. J.; North, M. Recent Developments in Organocatalysed Transformations of Epoxides and Carbon Dioxide into Cyclic Carbonates. *Green Chemistry* **2021**, *23* (1), 77-118, 10.1039/D0GC03465G.
(34) Jin, R.; Xu, H.; Easa, J.; Chapero-Planell, A.; O'Brien, C. P. Cycloaddition of CO_2 to Epichlorohydrin over Pyridine, Vinylpyridine, and Poly(vinylpyridine): The Influence of Steric Crowding on the Reaction Mechanism. *J. Phys. Chem. C* **2023**, *127* (3), 1441-1454.
(35) Qin, J.-J.; Chung, T.-S. Development of High-Performance Polysulfone/poly(4-vinylpyridine) Composite Hollow Fibers for CO_2/CH_4 Separation. *Desalination* **2006**, *192* (1), 112-116.
(36) Shieh, J.-J.; Chung, T. S. Gas Permeability, Diffusivity, and Solubility of Poly(4-vinylpyridine) film. *J. Polym. Sci. B Polym. Phys.* **1999**, *37* (20), 2851-2861.
(37) Soucy, T. L.; Dean, W. S.; Zhou, J.; Rivera Cruz, K. E.; McCrory, C. C. L. Considering the Influence of Polymer–Catalyst Interactions on the Chemical Microenvironment of Electrocatalysts for the CO_2 Reduction Reaction. *Accounts of chemical research* **2022**, *55* (3), 252-261.
(38) Abe, T.; Yoshida, T.; Tokita, S.; Taguchi, F.; Imaya, H.; Kaneko, M. Factors Affecting Selective Electrocatalytic CO_2 Reduction with Cobalt Phthalocyanine Incorporated in A Polyvinylpyridine Membrane Coated on a Graphite Electrode. *Journal of Electroanalytical Chemistry* **1996**, *412* (1), 125-132.
(39) Liu, Y.; McCrory, C. C. L. Modulating the Mechanism of Electrocatalytic CO_2 Reduction by Cobalt Phthalocyanine through Polymer Coordination and Encapsulation. *Nat. Comm.* **2019**, *10* (1), 1683.
(40) Ponnurangam, S.; Yun, C. M.; Chernyshova, I. V. Robust Electroreduction of CO_2 at a Poly(4-vinylpyridine)–Copper Electrode. *ChemElectroChem* **2016**, *3* (1), 74-82.
(41) Milella, F.; Mazzotti, M. Estimating Speciation of Aqueous Ammonia Solutions of Ammonium Bicarbonate: Application of Least Squares Methods to Infrared Spectra. *React. Chem. Eng.* **2019**, *4* (7), 1284-1302.
(42) Stegmeier, S.; Fleischer, M.; Tawil, A.; Hauptmann, P.; Egly, K.; Rose, K. Mechanism of the Interaction of CO_2 and Humidity with

Primary Amino Group Systems for Room Temperature CO_2 Sensors. *Procedia Chem.* **2009**, *1* (1), 236-239.
(43) Wen, N.; Brooker, M. H. Ammonium Carbonate, Ammonium Bicarbonate, and Ammonium Carbamate Equilibria: A Raman Study. *J. Phys. Chem.* **1995**, *99* (1), 359-368.
(44) Liu, J.; Yang, G.; Liu, Y.; Wu, D.; Hu, X.; Zhang, Z. Metal-Free Imidazolium Hydrogen Carbonate Ionic Liquids as Bifunctional Catalysts for the One-Pot Synthesis of Cyclic Carbonates from Olefins and CO_2. *Green Chemistry* **2019**, *21* (14), 3834-3838, 10.1039/C9GC01088B.
(45) Prajapati, A.; Sartape, R.; Galante, M. T.; Xie, J.; Leung, S. L.; Bessa, I.; Andrade, M. H. S.; Somich, R. T.; Rebouças, M. V.; Hutras, G. T.; et al. Fully-Integrated Electrochemical System that Captures CO_2 from Flue Gas to Produce Value-Added Chemicals at Ambient Conditions. *Energy Environ. Sci.* **2022**, *15* (12), 5105-5117, 10.1039/D2EE03396H.
(46) Welch, A. J.; Dunn, E.; DuChene, J. S.; Atwater, H. A. Bicarbonate or Carbonate Processes for Coupling Carbon Dioxide Capture and Electrochemical Conversion. *ACS Energy Letters* **2020**, *5* (3), 940-945.
(47) Xia, Q.; Zhang, K.; Zheng, T.; An, L.; Xia, C.; Zhang, X. Integration of CO_2 Capture and Electrochemical Conversion. *ACS Energy Letters* **2023**, *8* (6), 2840-2857.
(48) Freeman, B. D. Basis of Permeability/Selectivity Tradeoff Relations in Polymeric Gas Separation Membranes. *Macromolecules* **1999**, *32* (2), 375-380.
(49) Robeson, L. M. The Upper Bound Revisited. *J. Membr. Sci.* **2008**, *320* (1), 390-400.
(50) Robeson, L. M. Correlation of Separation Factor versus Permeability for Polymeric Membranes. *J. Membr. Sci.* **1991**, *62* (2), 165-185.
(51) Belaissaoui, B.; Lasseuguette, E.; Janakiram, S.; Deng, L.; Ferrari, M. C. Analysis of CO_2 Facilitation Transport Effect through a Hybrid Poly(Allyl Amine) Membrane: Pathways for Further Improvement. *Membranes (Basel)* **2020**, *10* (12).
(52) Klemm, A.; Lee, Y.-Y.; Mao, H.; Gurkan, B. Facilitated Transport Membranes With Ionic Liquids for CO_2 Separations. *Front. Chem.* **2020**, *8*, Mini Review.
(53) Guo, H.; Wei, J.; Ma, Y.; Deng, J.; Yi, S.; Wang, B.; Deng, L.; Jiang, X.; Dai, Z. Facilitated Transport Membranes for CO_2/CH_4 Separation - State of the Art. *Adv.Membr.* **2022**, *2*, 100040.
(54) Öztürk, T.; Yavuz, M.; Göktaş, M.; Hazer, B. One-step Synthesis of Triarm Block Copolymers by Simultaneous Atom Transfer Radical and Ring-opening Polymerization. *Polymer Bulletin* **2016**, *73* (6), 1497-1513.
(55) Shi, X.; Shi, H.; Wu, H.; Shen, H. Synthesis of Novel Perfluoroalkyl Ether Derivatives. *Research on Chemical Intermediates* **2018**, *44* (9), 5091-5105.
(56) Saikia, B. J.; Dolui, S. K. Designing Semiencapsulation Based Covalently Self-healable Poly(methyl methacrylate) Composites by Atom Transfer Radical Polymerization. *J. Polym. Sci., Part A: Polym. Chem.* **2016**, *54* (12), 1842-1851.
(57) Roshan, K. R.; Palissery, R. A.; Kathalikkattil, A. C.; Babu, R.; Mathai, G.; Lee, H.-S.; Park, D.-W. A Computational Study of the Mechanistic Insights into Base Catalysed Synthesis of Cyclic Carbonates from CO_2: Bicarbonate Anion as an Active Species. *Catal. Sci. Technol* **2016**, *6* (11), 3997-4004.

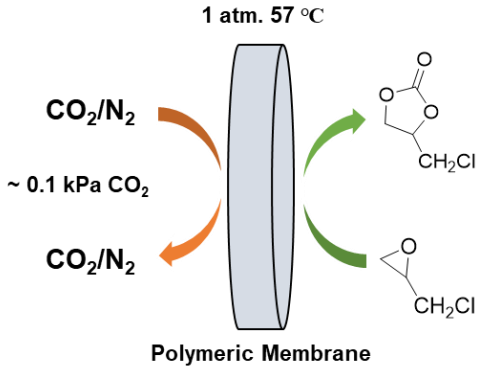

TOC